The University of Manchester Research

Monocular Visual-IMU Odometry: A Comparative Evaluation of the Detector-Descriptor Based Methods

DOI:
10.1007/978-3-319-46604-0_6

Document Version
Accepted author manuscript

Link to publication record in Manchester Research Explorer

Citation for published version (APA):
Dong, X., Dong, X., & Dong, J. (2016). Monocular Visual-IMU Odometry: A Comparative Evaluation of the Detector-Descriptor Based Methods. In G. Hua, & H. Jegou (Eds.), *Computer vision - ECCV 2016 workshops : Amsterdam, The Netherlands, October 8-10 and 15-16, 2016, proceedings* (Vol. Part 1, pp. 81-95). (Lecture Notes in Computer Science; Vol. 9913). Springer Nature. https://doi.org/10.1007/978-3-319-46604-0_6

Published in:
Computer vision - ECCV 2016 workshops

Citing this paper
Please note that where the full-text provided on Manchester Research Explorer is the Author Accepted Manuscript or Proof version this may differ from the final Published version. If citing, it is advised that you check and use the publisher's definitive version.

General rights
Copyright and moral rights for the publications made accessible in the Research Explorer are retained by the authors and/or other copyright owners and it is a condition of accessing publications that users recognise and abide by the legal requirements associated with these rights.

Takedown policy
If you believe that this document breaches copyright please refer to the University of Manchester's Takedown Procedures [http://man.ac.uk/04Y6Bo] or contact uml.scholarlycommunications@manchester.ac.uk providing relevant details, so we can investigate your claim.

Download date:25. Apr. 2024

Supplementary Material for ECCV 2016 Workshop Paper: Monocular Visual-IMU Odometry: A Comparative Evaluation of the Detector-Descriptor Based Methods

Xingshuai Dong [a], Xinghui Dong [b*], and Junyu Dong [a]

[a] Ocean University of China, Qingdao, 266071, China
[b] Centre for Imaging Sciences, University of Manchester, Manchester, M13 9PT, UK

Abstract. In Sections 1 to 5, we provide the figures of all the trajectories that are obtained in the five experiments introduced in the main paper. Each of these sections corresponds to a subsection of Section 5 in the main paper, i.e., an individual experiment. It should be noted that the figures shown here is not necessary for understanding the content of the main paper. In addition, we give the details of the five salient point detectors and eight local descriptors tested in this study and the configurations of five routes in Sections 6 and 7 respectively.

1 Route 1: Straight Line

In this section, five figures are displayed in terms of five different salient point detectors respectively. In each figure, the ground-truth trajectory (in black) and the estimated trajectories (in different colors) obtained using the IMU method and eight different local descriptors on the Straight Line route are shown together.

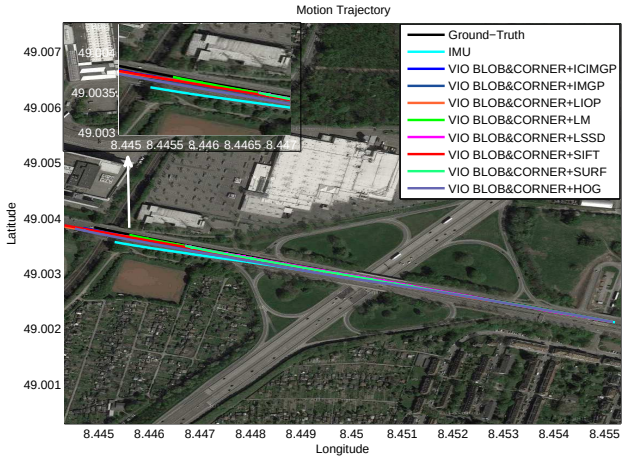

Fig. 1. The ground-truth motion trajectory and the trajectories obtained using IMU and the combinations of the Blob&Corner salient point detector and different local descriptors on the Straight Line route (express way, ≈780m, ≈60km/h). (Map source: GoogleEarth).

*Corresponding author: Xinghui Dong. Email: xinghui.dong@manchester.ac.uk.

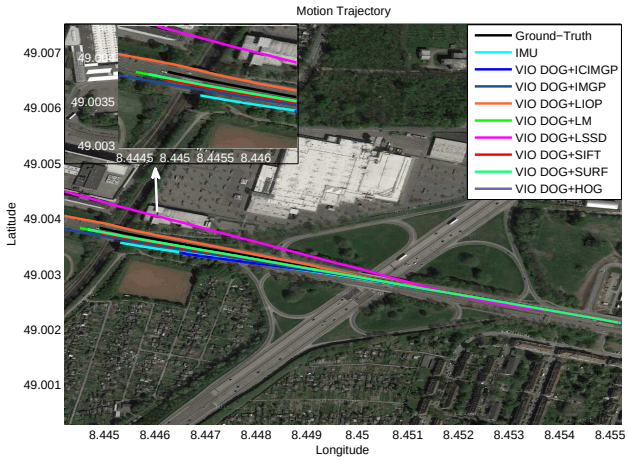

Fig. 2. The ground-truth motion trajectory and the trajectories obtained using IMU and the combinations of the DoG salient point detector and different local descriptors on the Straight Line route (express way, ≈780m, ≈60km/h). (Map source: GoogleEarth).

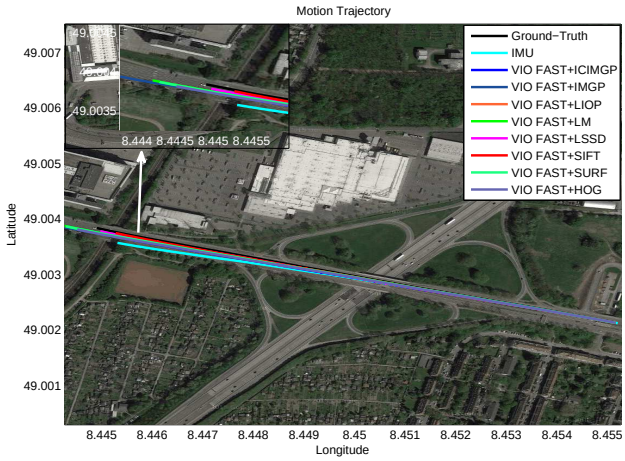

Fig. 3. The ground-truth motion trajectory and the trajectories obtained using IMU and the combinations of the FAST salient point detector and different local descriptors on the Straight Line route (express way, ≈780m, ≈60km/h). (Map source: GoogleEarth).

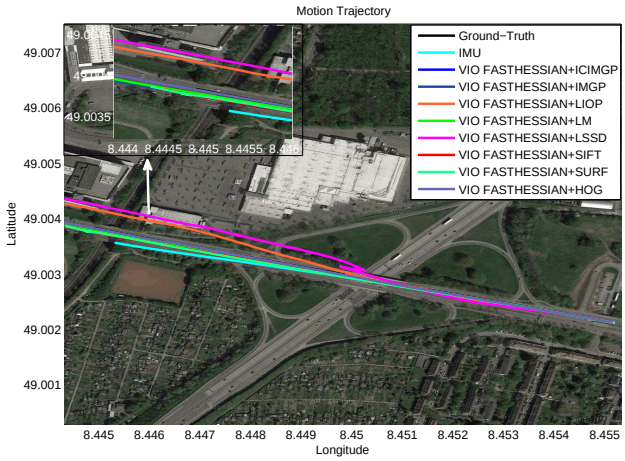

Fig. 4. The ground-truth motion trajectory and the trajectories obtained using IMU and the combinations of the Fast Hessian salient point detector and different local descriptors on the Straight Line route (express way, ≈780m, ≈60km/h). (Map source: GoogleEarth).

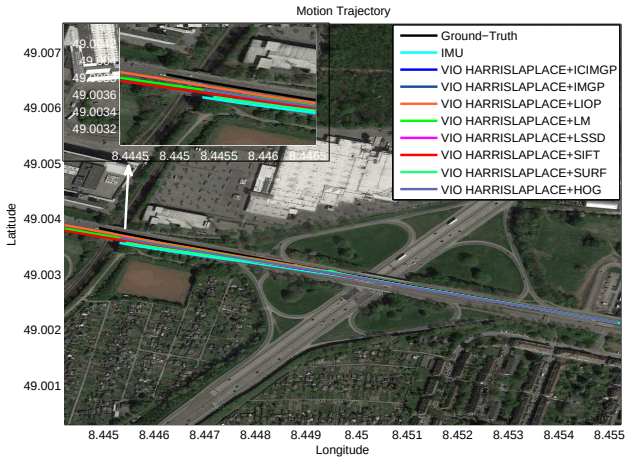

Fig. 5. The ground-truth motion trajectory and the trajectories obtained using IMU and the combinations of the Harris Laplace salient point detector and different local descriptors on the Straight Line route (express way, ≈780m, ≈60km/h). (Map source: GoogleEarth).

2 Route 2: Quarter Turn

This section shows five figures in terms of five different salient point detectors respectively. In each figure, the ground-truth trajectory (in black) and the estimated trajectories (in different colors) obtained using the IMU method and eight different local descriptors on the Quarter Turn route are shown together.

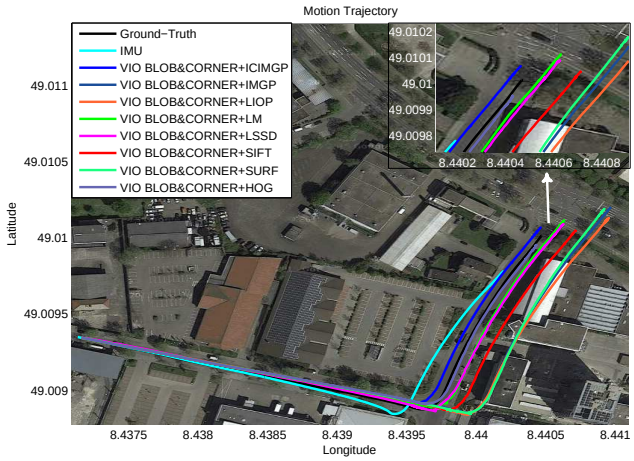

Fig. 6. The ground-truth motion trajectory and the trajectories obtained using IMU and the combinations of the Blob&Corner salient point detector and different local descriptors on the Quarter Turn route (urban road, ≈330m, ≈28km/h). (Map source: GoogleEarth).

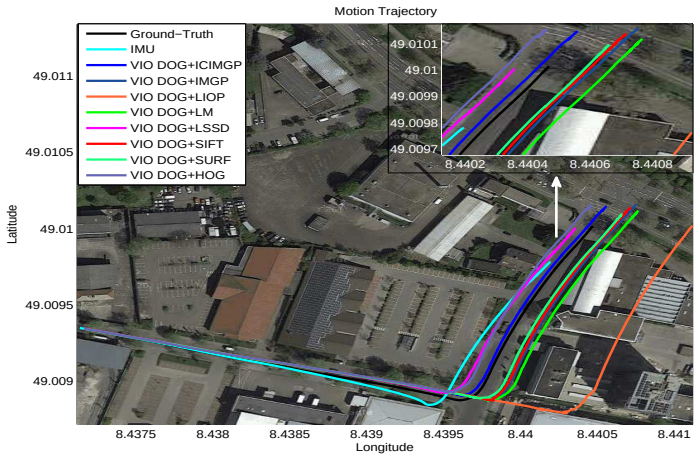

Fig. 7. The ground-truth motion trajectory and the trajectories obtained using IMU and the combinations of the DoG salient point detector and different local descriptors on the Quarter Turn route (urban road, ≈330m, ≈28km/h). (Map source: GoogleEarth).

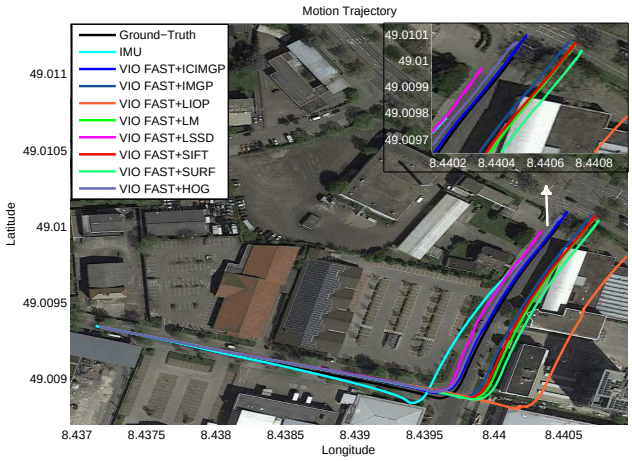

Fig. 8. The ground-truth motion trajectory and the trajectories obtained using IMU and the combinations of the FAST salient point detector and different local descriptors on the Quarter Turn route (urban road, ≈330m, ≈28km/h). (Map source: GoogleEarth).

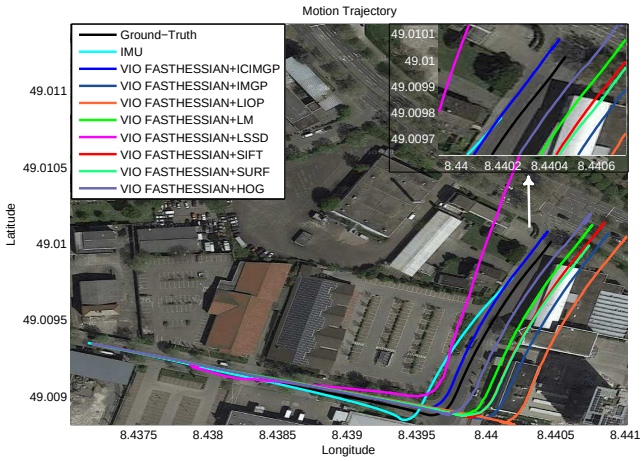

Fig. 9. The ground-truth motion trajectory and the trajectories obtained using IMU and the combinations of the Fast Hessian salient point detector and different local descriptors on the Quarter Turn route (urban road, ≈330m, ≈28km/h). (Map source: GoogleEarth).

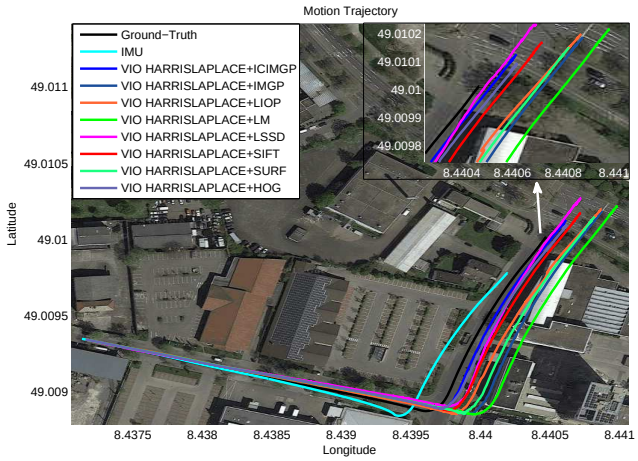

Fig. 10. The ground-truth motion trajectory and the trajectories obtained using IMU and the combinations of the Harris Laplace salient point detector and different local descriptors on the Quarter Turn route (urban road, ≈330m, ≈28km/h). (Map source: GoogleEarth).

3 Route 3: Multiple Quarter Turns

This section shows five figures in terms of five different salient point detectors respectively. In each figure, the ground-truth trajectory (in black) and the estimated trajectories (in different colors) obtained using the IMU method and eight different local descriptors on the Multiple Quarter Turns route are shown together.

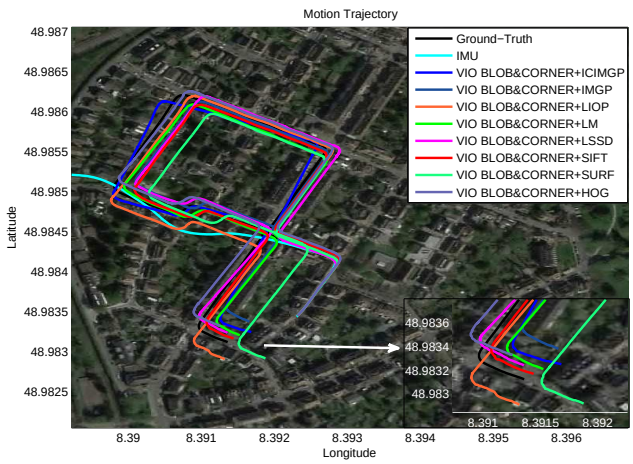

Fig. 11. The ground-truth motion trajectory and the trajectories obtained using IMU and the combinations of the Blob&Corner salient point detector and different local descriptors on the Multiple Quarter Turns route (residential area, ≈ 960m, ≈ 26km/h). (Map source: GoogleEarth).

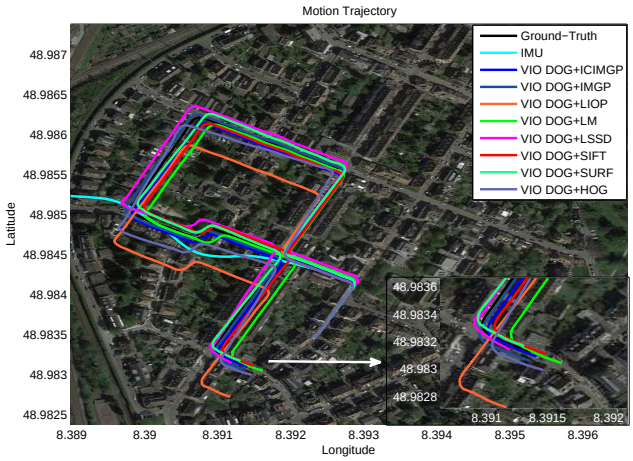

Fig. 12. The ground-truth motion trajectory and the trajectories obtained using IMU and the combinations of the DoG salient point detector and different local descriptors on the Multiple Quarter Turns route (residential area, ≈960m, ≈26km/h). (Map source: GoogleEarth).

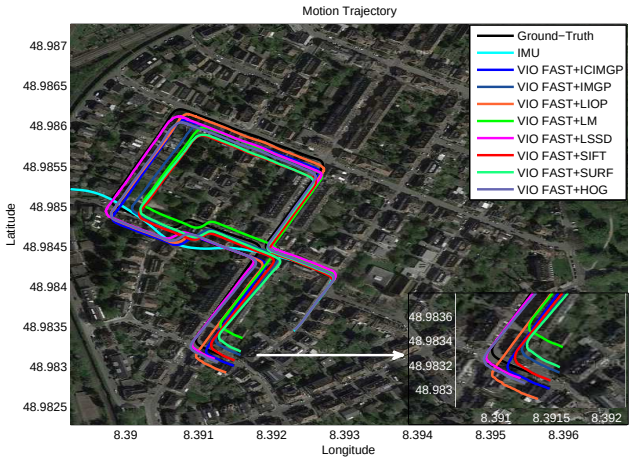

Fig. 13. The ground-truth motion trajectory and the trajectories obtained using IMU and the combinations of the FAST salient point detector and different local descriptors on the Multiple Quarter Turns route (residential area, ≈960m, ≈26km/h). (Map source: GoogleEarth).

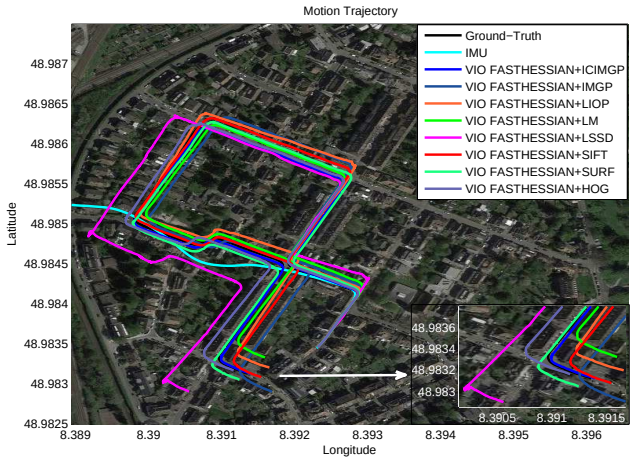

Fig. 14. The ground-truth motion trajectory and the trajectories obtained using IMU and the combinations of the Fast Hessian salient point detector and different local descriptors on the Multiple Quarter Turns route (residential area, $\approx$ 960m, $\approx$ 26km/h). (Map source: GoogleEarth).

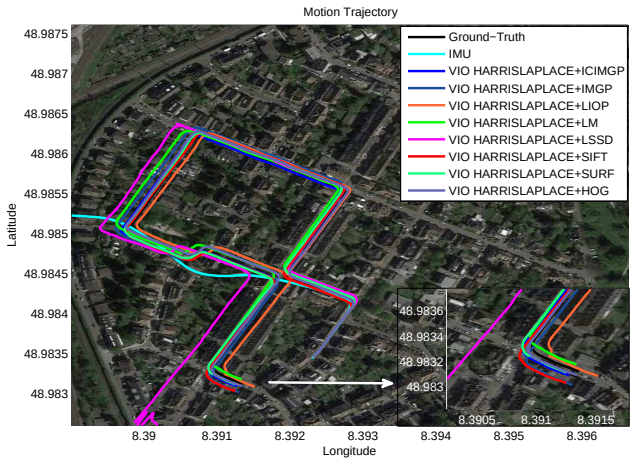

Fig. 15. The ground-truth motion trajectory and the trajectories obtained using IMU and the combinations of the Harris Laplace salient point detector and different local descriptors on the Multiple Quarter Turns route (residential area, $\approx$ 960m, $\approx$ 26km/h). (Map source: GoogleEarth).

4 Route 4: Multiple Curved Turns

In this section, five figures are displayed in terms of five different salient point detectors respectively. In each figure, the ground-truth trajectory (in black) and the esti-

mated trajectories (in different colors) obtained using the IMU method and eight different local descriptors on the Multiple Curved Turns route are shown together.

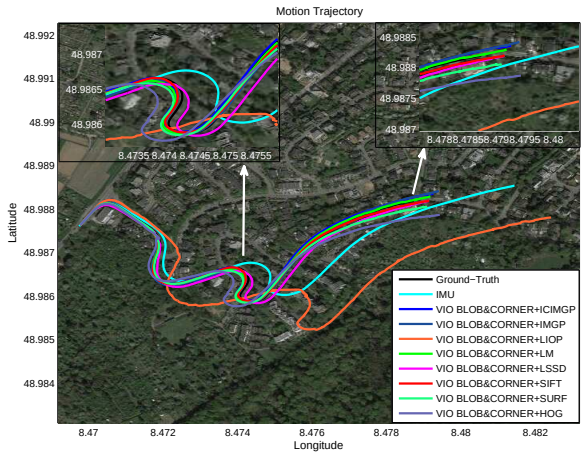

Fig. 16. The ground-truth motion trajectory and the trajectories obtained using IMU and the combinations of the Blob&Corner salient point detector and different local descriptors on the Multiple Curved Turns route (residential area, $\approx$ 1050m, $\approx$ 40km/h). (Map source: GoogleEarth).

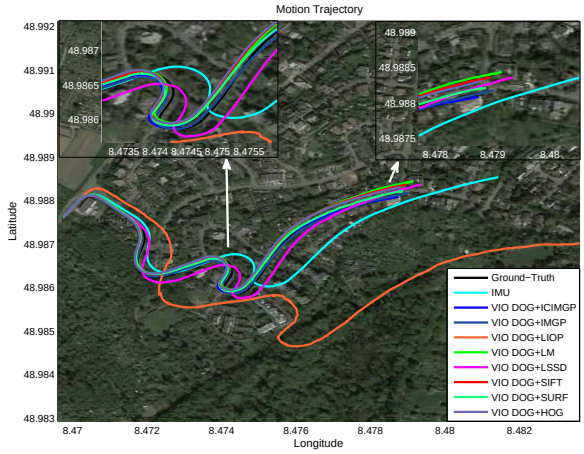

Fig. 17. The ground-truth motion trajectory and the trajectories obtained using IMU and the combinations of the DoG salient point detector and different local descriptors on the Multiple Curved Turns route (residential area, $\approx$1050m, $\approx$40km/h). (Map source: GoogleEarth).

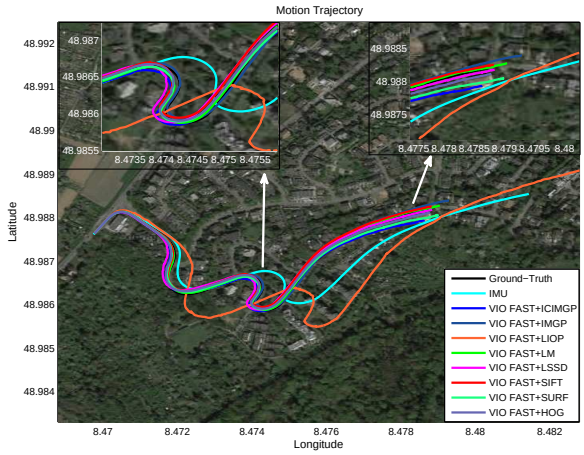

Fig. 18. The ground-truth motion trajectory and the trajectories obtained using IMU and the combinations of the FAST salient point detector and different local descriptors on the Multiple Curved Turns route (residential area, ≈1050m, ≈40km/h). (Map source: GoogleEarth).

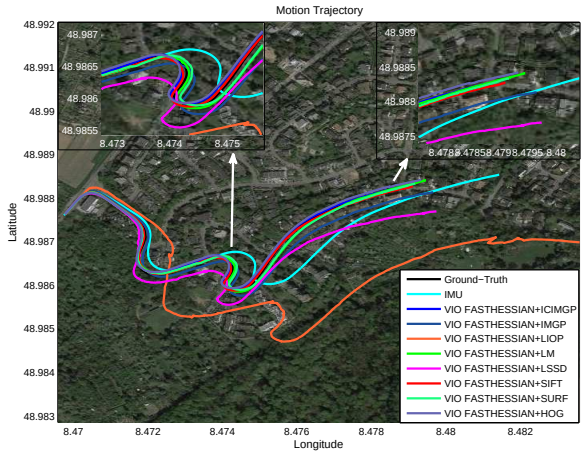

Fig. 19. The ground-truth motion trajectory and the trajectories obtained using IMU and the combinations of the Fast Hessian salient point detector and different local descriptors on the Multiple Curved Turns route (residential area, ≈ 1050m, ≈ 40km/h). (Map source: GoogleEarth).

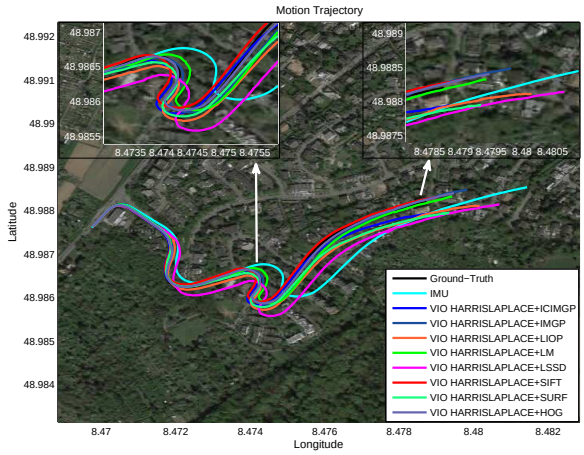

Fig. 20. The ground-truth motion trajectory and the trajectories obtained using IMU and the combinations of the Harris Laplace salient point detector and different local descriptors on the Multiple Curved Turns route (residential area, $\approx$ 1050m, $\approx$ 40km/h). (Map source: GoogleEarth).

5 Route 5: Loop Line

This section displays five figures in terms of five different salient point detectors respectively. In each figure, the ground-truth trajectory (in black) and the estimated trajectories (in different colors) obtained using the IMU method and eight different local descriptors on the Loop Line route are shown together.

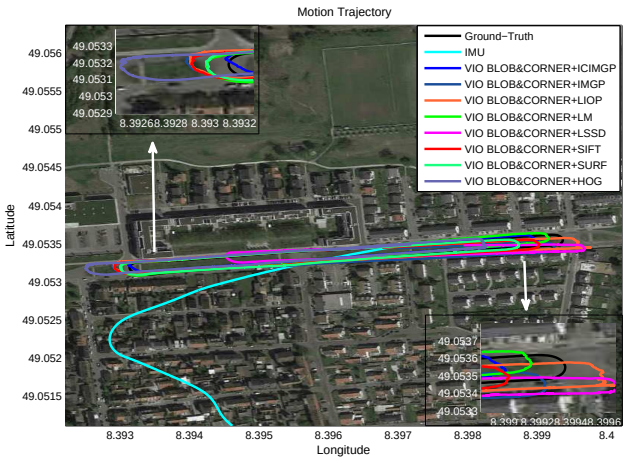

Fig. 21. The ground-truth motion trajectory and the trajectories obtained using IMU and the combinations of the Blob&Corner salient point detector and different local descriptors on the Loop Line route (residential area, $\approx$930m, $\approx$38km/h). (Map source: GoogleEarth).

Fig. 22. The ground-truth motion trajectory and the trajectories obtained using IMU and the combinations of the DoG salient point detector and different local descriptors on the Loop Line route (residential area, ≈930m, ≈38km/h). (Map source: GoogleEarth).

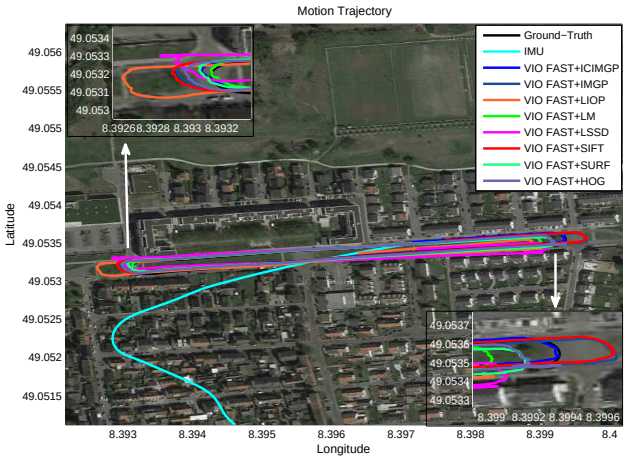

Fig. 23. The ground-truth motion trajectory and the trajectories obtained using IMU and the combinations of the FAST salient point detector and different local descriptors on the Loop Line route (residential area, ≈930m, ≈38km/h). (Map source: GoogleEarth).

Fig. 24. The ground-truth motion trajectory and the trajectories obtained using IMU and the combinations of the Fast Hessian salient point detector and different local descriptors on the Loop Line route (residential area, ≈930m, ≈38km/h). (Map source: GoogleEarth).

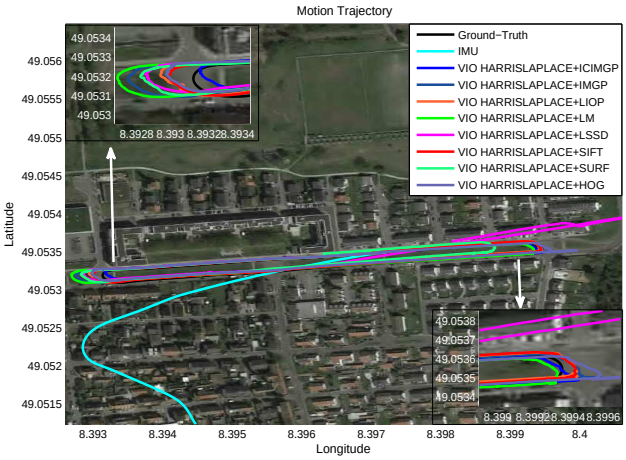

Fig. 25. The ground-truth motion trajectory and the trajectories obtained using IMU and the combinations of the Harris Laplace salient point detector and different local descriptors on the Loop Line route (residential area, ≈930m, ≈38km/h). (Map source: GoogleEarth).

6 Parameter Values of the Salient Point Detectors and Local Descriptors

In this section, we list the parameters used for the five salient point detectors and eight local descriptors in detail.

6.1 Parameter Values of the Salient Point Detectors

Detector	Parameter	Value
Blob&Corner	Window Size	13×13
DoG	Octaves	4
	Levels Per Octave	3
	σ_0	1.6
Fast Hessian	Octaves	4
	Threshold θ	0.2
	Sampling Step n	2
FAST	Threshold t	30
Harris-Laplace	Peak Threshold	0.000002
	Edge Threshold	10

6.2 Parameter Values of the Local Descriptors

Detector	Parameter	Value
HOG	Block Size	15×15
	Cell Size	5×5
	Number of Orientations	9
IMGP	Patch Size	11×11
ICIMGP	Number of Channels	8
	Patch Size	11×11
LM	σ_x	$\sqrt{2}$, 2, $2\sqrt{2}$
LIOP	Number of Spatial Bins	6
	Number of Neighbors	4
	Sampling Radius R	6
LSSD	Patch Size	5×5
	Region Radius	40
	n_r	12
	n_θ	3
SIFT	Sub-window Size	4×4
	Number of Bins Per Window	3
SURF	Window Size	4×4

7 Configurations of the Five Routes

We describe the details of each route used in this study in terms of the information provided with the KITTI dataset in the table below.

Route No.	Sequence No. in the KITTI Dataset	No. of the Start Point Image (The Left Color Camera Image)	No. of the End Point Image (The Left Color Camera Image)
1	2011_09_26_drive_0101_sync	0000000361	0000000816
2	2011_09_26_drive_0009_sync	0000000000	0000000405
3	2011_10_03_drive_0027_sync	0000000301	0000001610
4	2011_10_03_drive_0034_sync	0000000000	0000000899
5	2011_09_30_drive_0020_sync	0000000000	0000000834